2-1-2006

Estimating the Long-Term Hydrological Budget over Heterogeneous Surfaces

Jie Song

M.L. Wesely

D.J. Holdridge

D.R. Cook

J. Klazura

Estimating the Long-Term Hydrological Budget over Heterogeneous Surfaces

J. SONG

Department of Geography, Northern Illinois University, DeKalb, Illinois

M. L. WESELY,* D. J. HOLDRIDGE, D. R. COOK, AND J. KLAZURA

Environmental Research Division, Argonne National Laboratory, Argonne, Illinois

(Manuscript received 7 February 2005, in final form 1 August 2005)

ABSTRACT

Estimates of the hydrological budget in the Walnut River Watershed (WRW; ~5000 km^2) of southern Kansas were made with a parameterized subgrid-scale surface (PASS) model for the period 1996–2002. With its subgrid-scale distribution scheme, the PASS model couples surface meteorological observations with satellite remote sensing data to update root-zone available moisture and to simulate surface evapotranspiration rates at high resolution over extended areas. The PASS model is observationally driven, making use of extensive parameterizations of surface properties and processes. Heterogeneities in surface conditions are spatially resolved to an extent determined primarily by the satellite data pixel size. The purpose of modeling the spatial and interannual variability of water budget components at the regional scale is to evaluate the PASS model's ability to bridge a large grid cell of a climate model with its subgrid-scale variation. Modeled results indicate that annual total evapotranspiration at the WRW is about 66%–88% of annual precipitation—reasonable values for southeastern Kansas—and that it varies spatially and temporally. Seasonal distribution of precipitation plays an important role in evapotranspiration estimates. Comparison of modeled runoff with stream gauge measurements demonstrated close agreement and verified the accuracy of modeled evapotranspiration at the regional scale. In situ measurements of energy fluxes compare favorably with the modeled values for corresponding grid cells, and measured surface soil moisture corresponds with modeled root-zone available moisture in terms of temporal variability despite very heterogeneous surface conditions. With its ability to couple remote sensing data with surface meteorology data and its computational efficiency, PASS is easily used for modeling surface hydrological components over an extended region and in real time. Thus, it can fill a gap in evaluations of climate model output using limited field observations.

1. Introduction

Key issues in meteorology, climatology, and resource management deal with water in its various forms in the global water cycle. To investigate the water and energy budgets at various spatial and temporal scales, much research has been conducted on land–atmosphere exchanges in the Global Energy and Water-Cycle Experiment Continental-Scale International Project. Built on detailed surface physical processes, the advanced Oregon State University Land Surface Model (Mahrt and Ek 1984; Marht and Pan 1984; Pan and Mahrt 1987) was implemented by Chen and Dudhia (2001) in the fifth-generation Pennsylvania State University–National Center for Atmospheric Research (NCAR) Mesoscale Model (MM5) to describe land–atmosphere exchanges. Because of relatively large errors in modeled precipitation and unrealistic descriptions of land surface features, numerical models like this are used mostly for sensitivity studies, rather than for detailed investigations of water and energy budgets.

In recent decades, with the advancement of remote sensing technology and data processing, retrieval of water and energy fluxes from land surface models driven by satellite and surface observations has been more successful. For example, Anderson et al. (1997), Mecikalski et al. (1999), and Anderson et al. (2005) detailed a

* Deceased.

Corresponding author address: Jie Song, Dept. of Geography, Northern Illinois University, DeKalb, IL 60115.
E-mail: jsong@niu.edu

method for evaluating fluxes of sensible and latent heat at the land surface by using the Atmospheric Land Surface Exchange Inverse (ALEXI) model. This model is driven by Geostationary Operations Environmental Satellite (GOES)-derived surface brightness temperature changes and solar insolation, advanced very high resolution radiometer (AVHRR)-derived land cover properties, and synoptic weather and radiosonde data. The fluxes are computed at the end of a given day when GOES observations of surface radiometric temperature become available. Because the ALEXI model is driven primarily by data that can be obtained from remote sensing instruments, clear-sky condition, especially in the morning, is very important for the daily energy flux simulation. In addition, the assumption of a constant evaporative fraction during the day in ALEXI may not hold when weather changes during the day. Furthermore, observations from synoptic weather and radiosonde network are required for the atmospheric correction and model input. However, intensive and frequent radiosonde data are only available during expensive field experiments. Therefore, long-term as well as near-real-time modeling of surface water and energy fluxes at regional or large scale limit the model input to routine observations, which should be easily obtainable without lengthy processing.

In this study, our purpose is to address two major questions that are important for the current continental-scale water cycle study: 1) Can regional- and large-scale evapotranspiration, energy fluxes, and root-zone soil moisture over heterogeneous land surfaces be simulated accurately with routine surface and satellite observations over multiyear time scales and in nearly real time? 2) How can modeled evapotranspiration at the regional scale be evaluated reasonably across multiple years? The parameterized subgrid-scale surface flux (PASS) model, detailed in Song et al. (2000b), does not rely heavily on daily satellite input. It is driven primarily by routine, continuous surface meteorological observations, requiring remote sensing composite normalized-difference vegetation index (NDVI) values only at biweekly intervals. Thus, the PASS model enables the estimation of water and energy fluxes under all possible weather conditions.

Root-zone available soil moisture plays a key role in surface hydrological balances because it directly influences the surface evapotranspiration rate. Variations in evapotranspiration and runoff into streams and rivers cannot be fully assessed without knowledge of root-zone available moisture. However, obtaining accurate estimates of this quantity over large terrestrial areas can be difficult, because large temporal and spatial variability results from the unevenness of precipitation and the diversity of vegetation. Hirabayashi et al. (2001) proposed a method for estimating root-zone moisture content from surface soil moisture, which in turn is estimated by microwave remote sensing in the Global Soil Wetness Project. However, values need to be corrected for time lag and intensity of precipitation. Alternatively, the PASS model can be applied directly to estimate spatial and temporal variations in both evapotranspiration rate and root-zone available moisture (Song et al. 2000b).

To address the water cycle, the U.S. Department of Energy (DOE) initiated a 3-yr pilot study in the Walnut River Watershed (WRW), which encompasses an area of about 5000 km^2 in southeastern Kansas. The Whitewater Subbasin lies in the northwest region of the WRW. Work at the Argonne National Laboratory, one of five primary participants in the pilot study, included simulation of root-zone available moisture content and evapotranspiration in the WRW with the PASS model over multiyear period. In contrast, most short-term field experiments and modeling activities, such as the First International Satellite Land Surface Climatology Project (ISLSCP) Field Experiment (FIFE)-87 (Sellers et al. 1988); Cooperative Atmosphere–Surface Exchange Study (CASES)-97 (LeMone et al. 2000; Song et al. 2000b; Yates et al. 2001); Southern Great Plains (SGP-97) Hydrological Experiment (French et al. 2001), International H_2O Project (IHOP2002) (Weckwerth et al. 2004); Soil Moisture Atmospheric Coupling Experiment (SMACEX02; Anderson et al. 2003), have concentrated on the summer growing season, which lasts for only a few months, and at selected environmental conditions. Surface models verified with data from intensive experiments might perform less well in other seasons and during prolonged drought or wet conditions. The Atmospheric Boundary Layer Experiments (ABLE) site in southern Kansas, the first long-term site supported by DOE for studies of regional-scale water and energy budgets, has enabled the current multiyear modeling study of the water and energy budgets. One goal for long-term modeling of surface hydrological components at regional scales or at a grid scale suitable for high-resolution global climate models is to describe seasonal variations in surface hydrological variables accurately, even when the surface is spatially very heterogeneous. Another goal is to resolve the subgrid-scale variability of precipitation, soil moisture, and vegetation to the extent that biases are not introduced by the scheme of aggregating to computationally manageable grid cell sizes. To address these goals and to aid in the study of the interannual variability of key surface hydrological components, research continues on the ability of the PASS model to simulate available soil moisture and evapotranspiration in the WRW over the seven-year period of 1996–2002.

Field observations of soil moisture content are typically too limited to provide the spatial resolution and coverage required to describe the spatial heterogeneity of soil moisture adequately over extended areas. Song et al. (1997) modeled the influence of heterogeneous soil moisture on latent and sensible heat fluxes and found that simulated regional-scale latent heat fluxes tend to be higher and air temperatures lower under uniform surface conditions than under spatially heterogeneous conditions. Pitman et al. (1993) demonstrated that possible biases associated with the under representation of regional land surface heterogeneity within climate models might explain the propensity of climate models to overestimate grid-cell evapotranspiration and to underestimate runoff. This suggests that detailed information on the spatial distribution of the surface conditions appears to be necessary to simulate evapotranspiration accurately over extended areas. However, estimating surface fluxes at resolution higher than that of the climate model's grid cell can be difficult, because remote sensing data emphasize local land surface conditions, while the surface fluxes can be strongly influenced by surface–atmosphere interactions over substantially larger areas (Friedl 1996). The PASS model overcomes these limitations by coupling NDVI from satellite AVHRR data (at the climate model's subgrid-scale resolution) with surface meteorological observations in the study region (at the climate model's grid-scale resolution) to infer surface temperature, root-zone available moisture content, and evapotranspiration (at the climate model's subgrid scale, which is equivalent to the pixel resolution of the satellite used here).

The PASS model couples spatially sparse yet continuous data from meteorological stations with temporally sparse yet spatially highly resolved satellite remote sensing data to retrieve updated surface hydrological components over extended areas. Heterogeneities in surface conditions are spatially resolved to an extent determined primarily by the satellite data pixel size. Previous studies evaluated the model's ability during a relatively short intensive observation period (Song et al. 2000a,b). The present study evaluated long-term (multiyear) simulation of surface hydrological components by PASS modeling with continuous input of data from satellites, radars, and meteorological stations.

2. The PASS model

The original version of PASS model was developed by Gao (1995) and was applied by Gao et al. (1998). More recently, the model was improved by Song et al. (2000a,b) and evaluated with observations from an intensive field experiment. The PASS model uses a computationally efficient algorithm for computing subgrid-scale surface energy partitioning on the basis of an analytical solution to surface energy budget equations. An efficient computing algorithm is needed for long-term studies because of the large number of pixels associated with the satellite, land use, and soil characteristics data. A detailed description of the PASS model was provided by Song et al. (2000a,b). Here, the approach is briefly outlined, and additional requirements for long-term simulation are described.

All variables in the model are described at two scales: the regional scale of at least 100 km (a climate model's grid scale) and the satellite pixel scale (the climate model's subgrid scale). The regional-scale variables are approximated by the average of the observations made at the surface meteorological stations. Values of satellite pixel-scale surface parameters, including roughness length, surface albedo, surface conductance for water vapor, and the ratio of soil heat flux to net radiation, are estimated according to satellite-derived spectral indices and land use classes. These relationships contain empirical coefficients whose values have been derived for midlatitude areas with surface vegetation dominated by grasslands and agricultural crops. To account for the feedback of locally influenced meteorological conditions on the local atmosphere–surface exchange, pixel-specific near-surface meteorological conditions such as air temperature, vapor pressure, and wind speed are adjusted from their corresponding values at the regional scale according to local surface forcing as described below.

a. Model inputs

For seasonal and long-term studies, variations in vegetative condition and precipitation distribution must be considered. Thus, biweekly composite NDVI data and daily radar-based precipitation are required, along with regional incoming solar irradiance, surface air temperature, relative humidity, and wind speed observed continuously at surface meteorological stations in the area. Also required for PASS modeling are land cover data and available water capacity data from soil surveys.

b. Precalculation

Precalculation focuses on estimating pixel-specific aerodynamic surface temperature and region-representative surface temperature, both of which are needed to apply the distribution function for deriving air temperature at the pixel scale in the subsequent step. In the long-term surface hydrological study, aerodynamic surface temperatures are estimated at each time step in PASS with a second-order approximation involving the energy budget equation (Song et al. 2000b) because radiometric surface temperature is not available continuously from satellite observations and it also tends to overestimate the aerodynamic temperature.

c. Subgrid-scale distribution

One of the distinct features of the PASS model is spatial distribution of meteorological data per the method of Seth et al. (1994). The regional meteorological variables for wind speed, air temperature, and water vapor pressure are considered as mean values that are spatially distributed to individual pixels according to the surface dynamic conditions and the strength of the local vertical transfer at each time step. For example, wind speed that corresponds to a cropland pixel with a higher NDVI will be less than its regional mean value because of momentum dissipation by a locally rougher surface. Incoming solar irradiance at the regional scale is important input for the PASS model, needed to account the effects of clouds on the long-term energy and water budgets. The irradiance is distributed homogeneously at each pixel. Cloud patterns associated with frequent midlatitude cyclone systems can be represented better by observed incoming solar irradiance. The effects of short-lived cumulus clouds that pass over the region can also be accounted for, though not at the scale of individual pixels. For this long-term surface hydrological study at the regional scale, regional-scale contributions of pixel-scale fluxes were emphasized.

d. Surface conductance calculation

After the pixel-scale variables are estimated by using the distribution function, surface conductance at each pixel is calculated with pixel-specific vapor deficit and relative root-zone available moisture content, along with the most recent satellite NDVI data and photosynthetically active radiation (PAR). Examination of the relationship between PAR and solar irradiance with Surface Radiation Research Branch (SURFRAD) data (www.srrb.noaa.gov/surfrad/) and ABLE data for the year 2000 showed that the ratio of PAR to incident solar irradiance varies from 0.45 to 0.49 at midday to 0.9 at sunrise and sunset over the years. As a first approximation, PAR is assumed to be equal to half of the incident solar irradiance for each time step.

e. Energy fluxes

Latent heat flux for each pixel, estimated by using bulk aerodynamic expression at each pixel, is dependent on the difference between saturation vapor pressure at the pixel-specific surface temperature and air vapor pressure. Sensible heat flux is likewise estimated by using bulk aerodynamic expression. The net radiation is found from the radiation balance involving observed incoming solar radiation, together with parameterized values of albedo, incoming longwave irradiance, and outgoing longwave irradiance. Surface ground heat flux is parameterized as function of net radiation, NDVI, and solar zenith angle.

f. Updates to root-zone available moisture

The change in pixel-scale root-zone moisture content due to water loss by evapotranspiration and recharge by precipitation during each time step is computed for the root zone. Root-zone water loss through gravity is not considered. The updated values then become model input in the next time step for iterative calculation. The amount of water loss through evapotranspiration is integrated at each time step and summed at each pixel for evaluation of basin-scale hydrological budgets. Surface runoff is assumed to occur when the PASS model estimate of root-zone moisture exceeds the available moisture capacity. Groundwater recharge was not estimated, though it would have been in a more complex hydrology model. In addition, frozen soil is not currently modeled in PASS, and radar-observed precipitation is all treated as rainfall. These assumptions may limit the application of PASS model in unfrozen regions in the winter and in regions with temperate climate, such as the southern Great Plains.

Though the root-zone depth is a crucial variable, it is quite difficult to estimate accurately, because it is dependent on plant species and the stage of growth, which are not identified well by the information available to PASS. That is, only broad categories of vegetation are identified, and only the general state of the vegetation can be inferred on the basis of NDVI data from satellites. The current version of PASS assumes that root depth depends on land cover. The depth is set equal to 0.2 m for residential- and urban-related grassy areas, 0.6 m for cropland and rangeland, and 2 m for woodland. These values account for all-important land use classes (Song et al. 2000a). The depths might be too small to include the entire root zone of the vegetation, but they do include most of the roots (e.g., Jackson et al. 1996).

For water-covered surfaces, such as lakes and reservoirs, evaporation is equal to potential evaporation with zero surface resistance and unlimited water supply. In most cases, evaporative loss is greater than precipitation over these surfaces; the deficit is taken from runoff of the watershed to assume constant water supply.

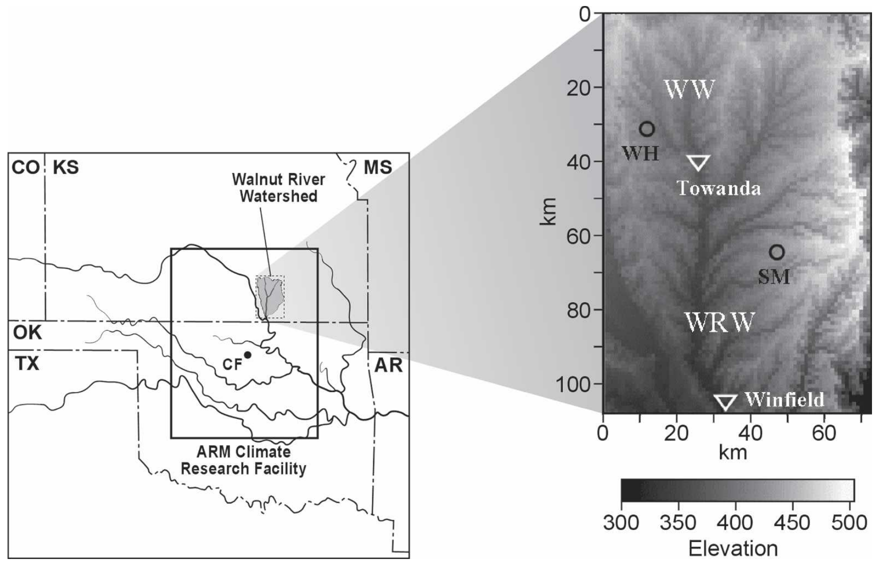

FIG. 1. Walnut River Watershed (WRW with outlet at Winfield) and Whitewater Watershed (WW with outlet at Towanda): geographic locations, topographic variations, and field sites at Whitewater and Smileyberg.

3. Site and data description

Located in southern Kansas, east of Wichita, the WRW is a rectangular region having an area of about 5000 km^2 within the Atmosphere Radiation Measurement (ARM) Climate Research Facility (Fig. 1). The WRW is representative of a global climate model's grid cell with heterogeneous land cover types. In addition to the large terrain gradient shown in Fig. 1, annual rainfall in the WRW varies from 76 cm in the west to 86 cm in the east, and average temperature varies from 0°C in the winter to 26°C in the summer (www.kwo.org/Org_People/walnut.htm). Land cover in the WRW is primarily a mix of grassland and cropland, with the cropland mostly in the western half of the basin. In addition to a few small scattered towns, Wichita suburbs expand into the western WRW. The Walnut River is the major stream, and the Whitewater River in the northwest is one of its tributaries. El Dorado Lake and Winfield Lake are major reservoirs on the river system. Surface water use for municipal, irrigation, recreational, and industrial purposes accounts for 91% of the water use in the basin (www.kwo.org/Org_People/walnut.htm). The WRW is a quasi-closed basin amenable to computing the components of the hydrological budget, and it is a tight watershed with minimum leakage into the substrata (LeMone et al. 2000). Nested within the northwest portion of the WRW is the 35 km × 30 km Whitewater Watershed (WW). These domains were selected for detailed observations and hydrological studies because of information provided by previous studies (LeMone et al. 2000).

a. Model input data

1) SATELLITE DATA

Simulations of evapotranspiration require descriptions of the spatial and temporal variations in surface vegetative conditions, especially those affecting bulk canopy stomatal conductance. Satellite remote sensing data can provide portions of the detailed information needed to drive some of the surface model parameterizations used to describe surface conditions. In particular, NDVI derived from the AVHRR on environmental satellites is a commonly used measure of surface greenness and associated surface properties. This study used biweekly composite 1-km-resolution NDVI values processed by the U.S. Geological Survey (USGS); the values of NDVI were adjusted with improved methods for compensating for atmospheric effects to estimate surface NDVI (DeFelice et al. 2002). Surface NDVI values were also obtained for the Whitewater (WH) and Smileyberg (SM) sites (Fig. 1) from measurements collected with a five-band Landsat Compatible Cropscan Multispectral Radiometer under high sun angles, taken in five or six samples over an area 200 m × 200 m at and around each site at biweekly intervals during the growing season.

The biweekly composite NDVI values derived from the National Oceanic and Atmospheric Administration (NOAA) AVHRR satellite represent values at each 1-km^2 pixel, while surface-observed NDVI values, which are shown as individual filled circles in Fig. 2, represent local point measurements (covering less than

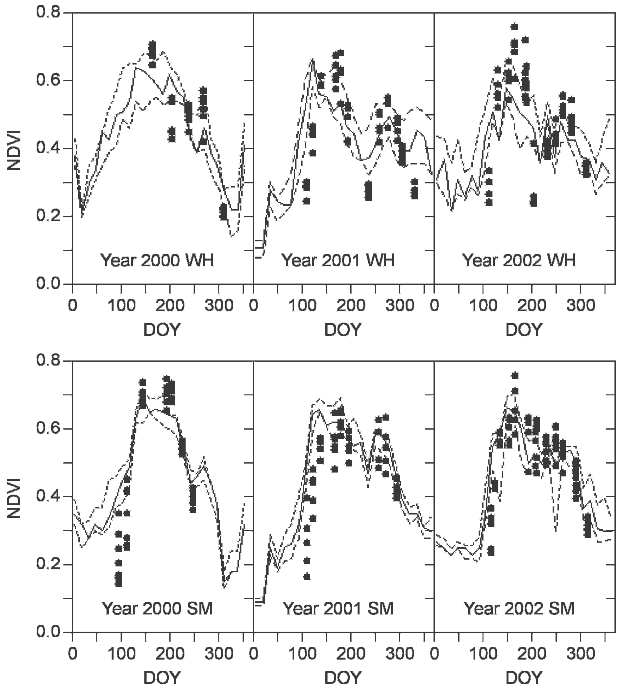

FIG. 2. Comparison of NDVI derived from satellite (solid lines) with in situ measurements (filled circles) at WH and SM. Upper and lower dashed lines around each solid line represent maximum and minimum NDVI, respectively, within a 3 km × 3 km area centered at each site.

10 m^2) randomly selected in an area of 200 m × 200 m. Because of surface heterogeneity, larger spatial variation is expected in locally measured NDVI values within an area 200 m × 200 m. Differences between NDVI derived from AVHRR and observed at the surface can be attributed to 1) scale differences, because surface measurements were taken at local points around the Whitewater site, while values from the satellite represent average NDVI within an area 1 km^2, that includes agricultural areas encompassing the Whitewater hayfield; 2) heterogeneity in surface conditions due to both soil characteristics and grazing at Smileyberg; and 3) time differences, with biweekly composite NDVI values derived from the satellite representing the largest NDVI within each two-week interval, while surface measurements are taken on a clear day within the same two-week interval. Despite the larger spatial variation in surface values than satellite values, the comparison in Fig. 2 indicates reasonable agreement in temporal variations. Because of the complexity in interpolating NDVI values at each biweekly interval, NDVI was assumed to be constant during each biweekly interval in the PASS modeling. Because the composite NDVI in each two-week period is the largest value for eliminating cloud contamination, input with constant biweekly composite NDVI values might lead to some overestimation in evapotranspiration during weeks of rapid growth. A study of the sensitivity of NDVI values to evapotranspiration indicated that observed biweekly NDVI in each year is necessary for accurate simulation of surface hydrology in the long term.

2) RADAR DATA

Regional Weather Surveillance Radar-1988 Doppler (WSR-88D) radar precipitation data were produced and disseminated by the National Weather Service's Arkansas–Red River Forecast Center. These radar-based rainfall estimates were evaluated independently by using a high-resolution network of rain gauges placed in the WRW as part of the DOE Atmospheric Boundary Layer Experiments (Miller et al. 2003). Rain gauge data from ABLE were compared to the Arkansas–Red River Forecast Center's radar-based estimates by using a nearest neighbor approach. Results show generally good agreement (within 20%) between these two independent rainfall estimates over the WRW. Given the overall quality of these results, the radar-based estimates for the entire Atmospheric Radiation Measurement Climate Research Facility are assumed to be of equally high quality.

Precipitation data in the WRW consisted of Hydrological Rainfall Analysis Project 4-km-resolution data, adjusted with rain gauge observations and supplied by the Arkansas–Red River Basin Forecast Center, which provides 24-h cumulative rainfall amount daily. As required for the PASS model, in the absence of 30-min precipitation data precipitation was assumed to be evenly distributed at 1200–2400 Central Standard Time (CST). This assumption is based on the general observation that precipitation tends to occur in the afternoon and evening hours in spring and summer. In addition, within each 4 km × 4 km area of radar resolution, precipitation was assumed to be homogeneously distributed.

3) LAND AND SOIL DATA

The land cover data were derived from the Kansas Applied Remote Sensing Program (data available online at http://www.epa.gov/OWOW/watershed/landcover/lulcusa.html), which performed the derivation from an unsupervised classification of Landsat Thematic Mapper data. The original data files contain information with a resolution of 30 m, from which land cover data of 1-km resolution were derived by taking the dominant land cover type.

Data on available water capacity at a resolution of 1 km were extracted from datasets based on county soil survey manuals (SSURGO 1995). The texture classes of soil in the WRW are mostly silt loam in the hills in the east and the central lowlands, and silty clay loam on the western uplands.

4) Surface data

Data on solar irradiance, air temperature, relative humidity, and wind speed were obtained as 30-min averages from surface stations operated by DOE's ARM Program and by ABLE in the WRW. The seven-year dataset was constructed mostly from observations at the ARM extended facility near Towanda (Fig. 1). Occasional gaps in the observational data were filled with data from nearby ARM extended facilities or by interpolation or extrapolation of data on days with similar environmental conditions. These meteorological measurements were used as the regionally representative values needed in the PASS model.

For the current study, a resolution of 1 km was chosen as the PASS model grid size; this is compatible with the scale of satellite AVHRR pixel. The original high-resolution land-use data files were aggregated spatially to 1-km-resolution files. Table 1 summarizes the spatial and temporal resolutions of the PASS model input data. The satellite remote sensing data were used to describe the surface vegetative conditions with biweekly composite, 1-km-resolution NDVI data products. The 4-km-resolution radar-based estimates of daily precipitation also constituted major input. Land use, root-zone depth, and available soil water capacity were assigned to each 1-km-resolution pixel. Local surface observations on downwelling solar irradiance, air temperature, relative humidity, and wind speed provided the driving force for modeled evapotranspiration. Regionally representative values of these parameters were estimated from regional meteorology stations and from ARM Program extended facilities in and around the WRW. Continuous meteorological observations made by ABLE in the WRW were coupled with daily radar-observed precipitation and biweekly composite NDVI to implement the PASS model.

Tests with a 200-m model grid—with land cover and available water capacity aggregated to 200-m-resolution and 1-km-resolution NDVI distributed homogeneously to 200-m pixels—revealed only small differences in modeled hydrological components at 200-m versus 1-km resolution, despite a greater computational demand at 200-m resolution.

On the first day of the first year, initial root-zone available soil moisture at each model grid was assumed to be at capacity; this is close to reality, because soil is typically near saturation at the end of each year.

b. *Data for model evaluation*

Traditional in situ evaluations for modeled water and energy fluxes are always complicated by comparison at different scales. Modeled values for an individual grid cell generally represent a larger area than can be represented by in situ observations. On the other hand, streamflow contributed from upstream tributaries and influenced mostly by precipitation and evapotranspiration in a basin can be used to evaluate evapotranspiration at the scale of a large watershed. In this study, besides the traditional comparison of water and energy fluxes at a few observational sites, streamflow measured at outlet gauges was used as a benchmark to evaluate whole-watershed runoff as one of the key water budget components.

Daily discharge data were obtained at two gauge stations operated by the USGS, with one gauge located at the outlet of the WRW near Winfield and the other one located at the subbasin WW outlet near Towanda (Fig. 1). The discharge data do not constitute inputs to PASS modeling, but they can be compared to runoff estimates. In PASS, runoff estimates are equivalent to excess water from the root zone.

An energy balance Bowen ratio station has been in operation at the WH site since mid 1999. Net radiation and latent, sensible, and ground heat fluxes have been measured, in addition to conventional surface meteorological observations. An eddy correlation (ECOR) station at the SM site has also taken measurements of latent and sensible heat fluxes. To overcome the underestimation of energy fluxes by the eddy correlation method, net radiation, and ground heat flux sensors were installed. Latent and sensible heat fluxes were adjusted to close the surface energy budget while keep-

TABLE 1. Resolution of input data for the PASS model.

Data	Source	Spatial resolution (km)	Temporal resolution
NDVI	NOAA AVHRR	1	Biweekly
Precipitation	Radar	4	Daily
Land cover	Kansas USGS	1	Permanent
Available water capacity	Soil Survey Geographic Database (SSURGO)	1	Permanent
Meteorology	Surface stations	~50	30 min

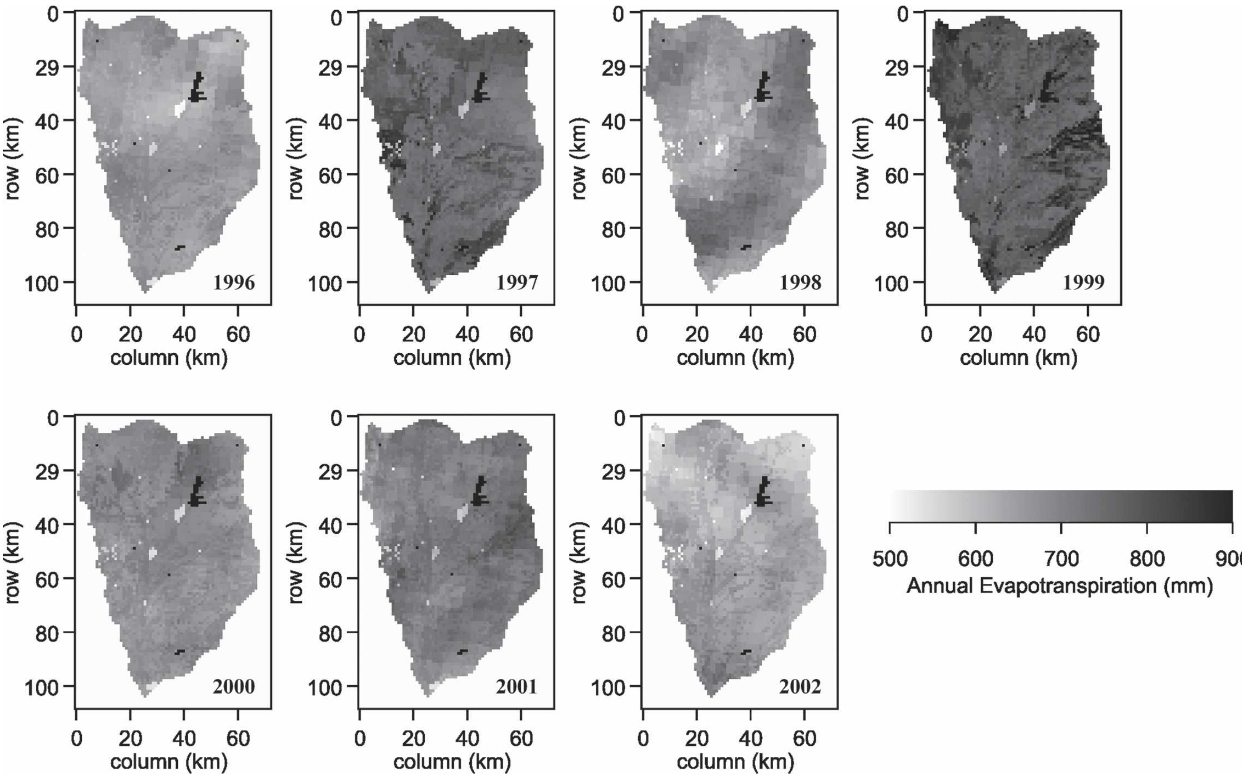

FIG. 3. Spatial patterns of modeled evapotranspiration accumulated in 1996–2002. Areas with largest evaporation are the El Dorado Lake reservoir (northeast) and the Winfield Lake reservoir (central south).

ing Bowen ratio constant. To account for the storage of soil heat between the surface and the ground heat sensor, gravimetric soil moisture in the surface layer (at depth of 0–5 cm) was also measured at both sites. PASS model estimates of surface water and energy fluxes can be verified with these local measurements.

4. Results of surface hydrological modeling

The PASS modeling was performed over a rectangular domain 73 km × 109 km, encompassing the WRW. The model resolution was 1 km (Fig. 1). Modeled outputs at each pixel within the WRW were selected for analysis. Spatial distributions of modeled evapotranspiration in 1996–2002 are displayed in Fig. 3. Within the WRW, modeled evaporative loss was largest above water surfaces (darkest areas) and smallest over urban and suburban (lightest) areas. Evapotranspiration in the WRW is very heterogeneous spatially, even when values are summed for each year. Table 2 summarizes annual values of modeled evapotranspiration and runoff for the total domain, as well as observed precipitation and streamflow for the WRW and subbasin WW. Evapotranspiration was largest in 1999, followed by 1997, and was smallest in 2002.

Seasonal variations in modeled evapotranspiration and root-zone available moisture are shown with observed precipitation in Fig. 4. The modeled root-zone available moisture shows an annual wet and dry cycle. In the summer, the large loss from evapotranspiration exceeds the moisture input from precipitation corre-

TABLE 2. Annual water budget in the Walnut River Watershed and the Whitewater Watershed.

	Water budget ($\times 10^9$ m^3)			
Year	Precipitation observed	Evaporation modeled	Runoff modeled	Streamflow observed
Walnut River watershed				
1996	3.60	3.16	0.51	0.37
1997	4.45	3.64	0.89	1.12
1998	5.05	3.31	1.63	1.81
1999	5.31	3.82	1.50	1.70
2000	4.49	3.37	1.09	0.82
2001	3.97	3.46	0.96	0.76
2002	4.34	3.07	0.86	0.63
Total	31.22	23.83	7.45	7.21
Whitewater watershed				
1996	0.82	0.73	0.10	0.07
1997	1.01	0.86	0.18	0.27
1998	1.21	0.76	0.43	0.44
1999	1.26	0.90	0.35	0.33
2000	1.02	0.79	0.22	0.11
2001	0.88	0.79	0.20	0.19
2002	0.87	0.69	0.09	0.08
Total	7.06	5.52	1.57	1.50

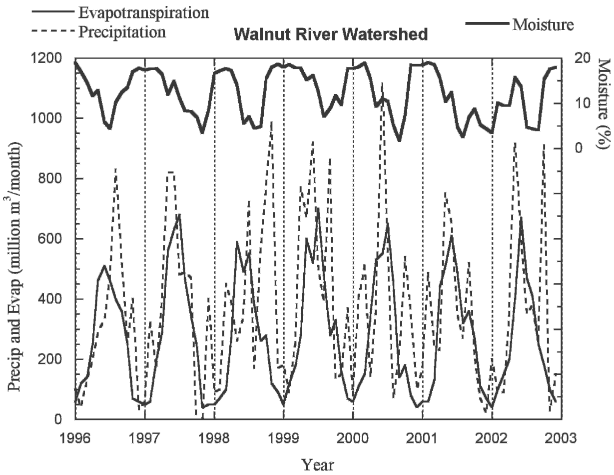

FIG. 4. Basin-scale observed precipitation and modeled evapotranspiration, with modeled mean root-zone available moisture.

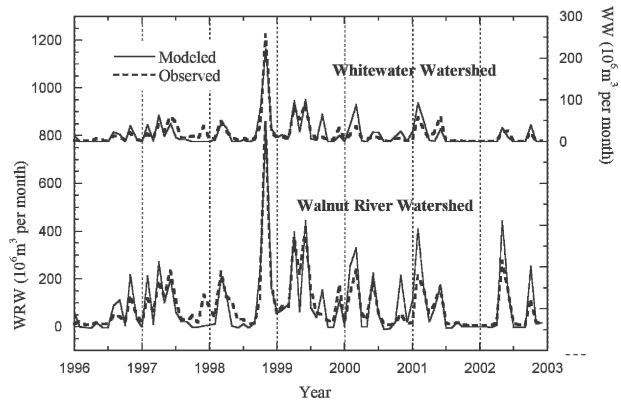

FIG. 5. Comparison of modeled runoff and stream gauge observations at the Winfield station for the Walnut River Watershed and at the Towanda station for the Whitewater Watershed.

sponding to the growing season. The wet periods at the end of each year reflect the reduction in evapotranspirative loss and the recharge from precipitation. An exception is the year 2001, when precipitation recharge was minimal after the growing season. In each year, precipitation was unevenly distributed; most rain fell in the warm growing season, except in 2002 (Fig. 4). The low modeled total evapotranspiration in 2002 is due to the timing of the rainfall as well as lower NDVI. Precipitation events in 2002 occurred mostly in spring and fall, rather than in the summer peak growing season (Fig. 4). With drier soil, vegetation did not grow well, as indicated by lower NDVI values, and thus evapotranspiration was limited. Similarly, in 1996, modeled evapotranspiration was next to lowest, because a prolonged dry period in the spring and early summer influenced both soil moisture and vegetation growth. In comparison, the largest modeled evapotranspiration, in 1999, corresponded to abundant precipitation during the entire growing season. In 1998, although annual total precipitation was greater than in 1999, modeled evapotranspiration was lower (Table 2), because relatively less rain fell during the summer growing season, leading to lower soil moisture and lower NDVI. Although the heaviest precipitation occurred later in the year 1998, evapotranspiration did not increase much after the growing season.

To evaluate modeled evapotranspiration over the extended heterogeneous region, we compared modeled runoff with the stream-gauge-measured streamflow (Fig. 5). Modeled runoff at each pixel was estimated as the excess soil water over capacity, and the values were summed for both the WRW and the WW subbasin. The Winfield stream gauge measures runoff integrated over the whole WRW; the Towanda stream gauge measures flow from the WW subbasin (Fig. 1). Figure 5 shows generally good correlation between modeled runoff and measured streamflow. At times, when the model assumptions are best satisfied, agreement is excellent. An example is in 1998, when a large amount of precipitation saturated the soil. At other times the agreement is not so good. An example of this is in early 2000 and 2001, when some of the precipitation might have occurred as snow. Modeled runoff exceeds observed streamflow in some of the high-flow periods but is less than the observed value during some low-flow periods. This may be explained by reservoir regulation and storage pond and is examined further below. The overall correlation values between modeled runoff and observed streamflow for the WRW and the WW are 0.91 and 0.89, respectively, with significance at 0.05.

Over the seven-year period shown in Table 2 for both the WRW and the WW, precipitation amounts varied greatly from dry years (e.g., 1996) to wet years (e.g., 1999). The modeled water loss due to evapotranspiration in the WRW varied from 66% (1998, a wet year) to 88% (1996, a dry year) of precipitation at the end of each year, which is reasonable for southern Kansas. The differences between the observed discharge and modeled runoff are small in comparison with precipitation amount. Modeled runoff amounts exceeded observed streamflow in years when annual precipitation was relatively low, such as 1996, 2001, and 2002. Modeled runoff was less than observed streamflow in years when annual precipitation was relatively high, such as 1998 and 1999. At the end of the seven-year period, the overall modeled runoff in the WRW was about 3% more than observed streamflow (5% for the WW subbasin).

Runoff comparisons can provide an evaluation of the regional-scale water budget, and comparisons with available field measurements can provide evidence for model performance at the pixel or local scale. In addition, the possibility that underestimation in modeled evapotranspiration resulted in increased modeled runoff during years 2000–2002 can be evaluated with in situ observations. Modeled latent heat fluxes and net radiation at the pixels nearest the WH and SM sites are compared in Fig. 6 with corresponding in situ observations during 2000–2002. Results indicate that modeled net radiation and latent heat fluxes are similar to the observations. On average, modeled net radiation is 11 (WH) and 24 W m^{-2} (SM) below the observed values, but modeled latent heat fluxes are only 2 (WH) and 8 W m^{-2} (SM) more than the observed values. Modeled sensible and ground heat fluxes are below the corresponding observations (data not shown), with average differences of 16 (WH) and 3 W m^{-2} (SM) for sensible heat and 1 (WH) and 2 W m^{-2} (SM) for ground heat.

The above evaluation of in situ latent heat fluxes indicates that the reason for greater modeled runoff than observed streamflow during years 2000–02 was not due to the underestimation of evapotranspiration within the watershed. In fact, evapotranspiration may have been overestimated slightly when biweekly composite NDVI was used instead of daily NDVI. To explain the possible cause of less observed than modeled runoff during the peak flow periods shown in Fig. 5, we further examined surface water usage in the WRW and found that water stored in the two major reservoirs in the WRW during the high-flow episodes was later withdrawn for municipal and irrigation purposes (Miller et al. 2005). The larger El Dorado Reservoir (Fig. 3) especially dominates water flow in the lower section of the Walnut River, because the river is fed primarily by water released from the reservoirs. At a smaller scale, collection of detailed sets of precipitation, stream, and soil water samples from a small tributary of the Whitewater River (the Rock Creek drainage basin) in May of 2002 (Miller et al. 2005) showed that the upper 30% of the drainage basin feeds into a stock pond that limits flow to the lower part of the creek to periods following precipitation events. Thus, in addition to snow accumulation, which can delay surface runoff in the spring, runoff storage in reservoirs and stock ponds in the upper part of the river drainage can cause observed streamflow to be less than modeled flow during a high-flow period but more than modeled flow during a low-flow period, as Fig. 5 shows. In addition, groundwater recharge is not modeled or measured, leaving the accounting for water loss incomplete.

Interannual and seasonal variations in modeled root-zone available moisture have shown reasonable trends

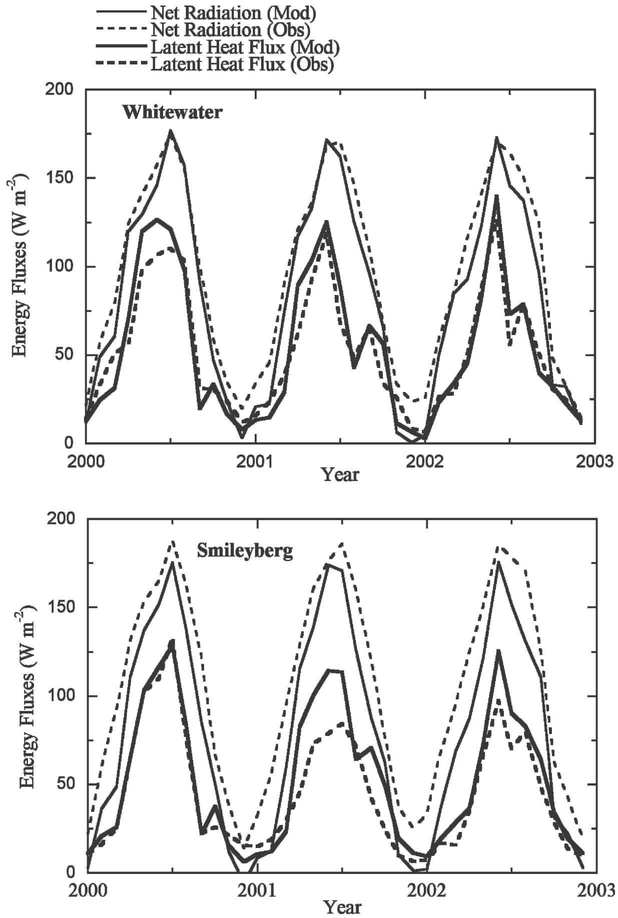

FIG. 6. Comparison of energy fluxes (modeled vs observed) at the Whitewater site and the Smileyberg site.

within the WRW. Evaluation is problematic because of a lack of observations at root-zone depth, although near-surface (at 2.5 cm) soil moisture has been measured at the WH and SM sites to account for heat storage for a ground heat flux correction. As a result, large differences are expected when comparisons are made between modeled root-zone available moisture at the pixels nearest the WH and SM sites and in situ surface soil moisture measurements (Fig. 7). The first reason for the difference between modeled and observed values is that unlike the observed total soil moisture content, modeled values are available moisture content, which does not include soil water that is not accessible at wilting point. In contrast, the observed values are not limited to available soil water. Second, modeled values represent the root-zone condition, which tends to be less extreme than surface conditions and does not respond to dryness and wetness as quickly as the observed surface condition. Third, because heterogeneity in soil texture and soil moisture is large, sampling even at five points within an area of about 4 m^2 at each site

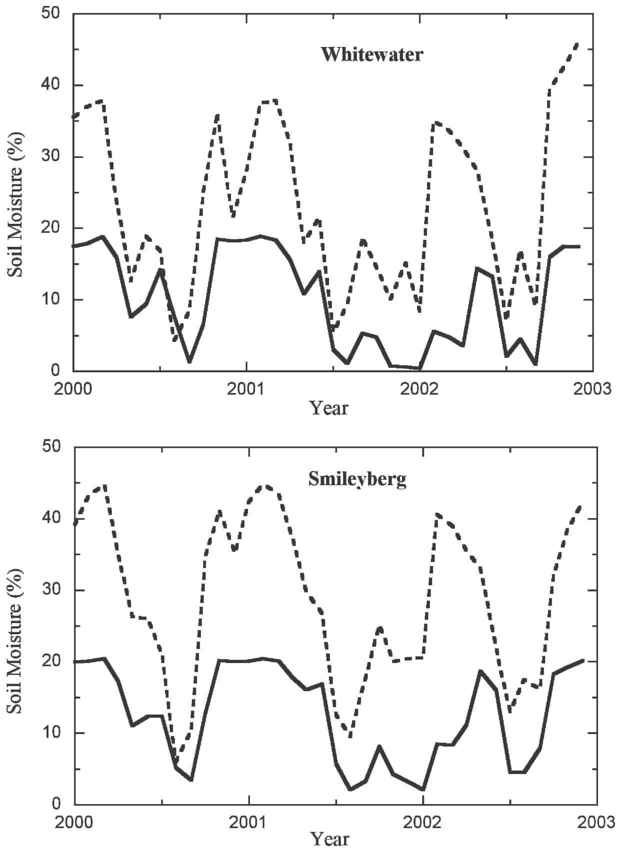

FIG. 7. Comparison of monthly averaged root-zone available moisture (modeled; solid line) and near-surface gravimetric soil moisture (measured; dashed line) at the Whitewater site and the Smileyberg site. The monthly values (36 samples) have correlation coefficients of 0.73 and 0.82 for Whitewater and Smileyberg, respectively.

might not adequately represent root-zone available moisture modeled at 1-km resolution. Fourth, heterogeneous soil texture requires calibration functions for moisture sensors to be generated by a field scientist for each site. Soil at SM soil is silty clay (bulk density 1.22, porosity 54%), while soil at WH is clay loam (bulk density 1.33, porosity 50%). The soil moisture values are adjusted according to nonlinear functions fitted to collected soil samples in a limited moisture range. Despite the difference between the modeled and observed values, temporal variations in the monthly averaged measurements shown in Fig. 7 are similar to those in modeled root-zone values, which sometimes lag behind the measured surface values because response is slower at root-zone depth.

5. Summary and conclusions

Estimates of evaporative water loss and root-zone available moisture in the WRW and WW were made with the PASS model and applied in an evaluation of hydrological balance components for 1996–2002. Satellite remote sensing data in biweekly composite, 1-km-resolution NDVI data products were used to describe the surface vegetative conditions. In addition, 4-km-resolution radar-based estimates of precipitation constituted major input. Surface radiation and basic meteorological data provided the driving force for modeling evapotranspiration.

The small differences between modeled runoff and observed streamflow, which is less than 5% for the seven-year period, indicates that the regional-scale surface evapotranspiration modeled by PASS is realistic, with errors of 10% or less. Seasonal changes in modeled evapotranspiration in years 2000–02 matched fairly well with the in situ flux measurements, with slight overestimates during certain seasons. Overall, modeled water and energy fluxes closely reflected observed spatial and long-term temporal variations in the region. The results suggest that a highly parameterized but relatively simple surface model like PASS can be exercised efficiently to estimate both real-time and long-term surface energy fluxes and hydrological components. Moreover, with its subgrid-scale resolvability, PASS can provide scale linkage for evaluating each grid cell of global climate models with regional streamflow measurements and field observations. Work continues on selection of proper root-zone depths for various types of vegetation.

Acknowledgments. This work was supported by the DOE Office of Science, Office of Biological and Environmental Research, Environmental Sciences Division, under Contract W-31-109-ENG-38, to Argonne National Laboratory, as part of the ARM Program. Contributors to this study included John Lucas, and Timothy Martin of Argonne National Laboratory and Charles Schaffer of Northern Illinois University.

REFERENCES

Anderson, M. C., J. M. Norman, G. R. Diak, W. P. Kustas, and J. R. Mecikalski, 1997: A two-source time-integrated model for estimating surface fluxes using thermal remote sensing. *Remote Sens. Environ.*, **60,** 195–216.

——, ——, W. P. Kustas, J. H. Prueger, C. Neale, I. Macpherson, J. Mecikalski, and G. Diak, 2003: Comparison of aircraft- and tower-measured fluxes acquired during Smacex with predictions from a regional atmosphere–land exchange model. Preprints, *17th Conf. on Hydrology*, Long Beach, CA, Amer. Meteor. Soc., CD-ROM, 1.7.

——, ——, ——, F. Li, J. H. Prueger, and J. R. Mecikalski, 2005: Effects of vegetation clumping on two-source model estimates of surface energy fluxes from an agricultural landscape during SMACEX. *J. Hydrometeor.,* **6,** 892–909.

Chen, F., and J. Dudhia, 2001: Coupling an advanced land–surface/hydrology model with the Penn State/NCAR MM5 modeling system. Part I: Model implementation and sensitivity. *Mon. Wea. Rev.,* **129,** 569–585.

DeFelice, T. P., D. Lloyd, D. J. Meyer, T. T. Baltzer, and P. Piraino, 2002: Water vapor correction of the daily 1-kilometer AVHRR global land data set. Part I: Validation and use of the water vapor input field. *Int. J. Remote Sens.,* **24,** 2365–2375.

French, A. N., T. J. Schmugge, and W. P. Kustas, 2001: Heat flux distributions over SGP97 sites. *Proc. Remote Sensing and Hydrology*, Santa Fe, NM, IAHS, 187–191.

Friedl, M. A., 1996: Relationships among remotely sensed data, surface energy balance, and area-averaged fluxes over partially vegetated land surfaces. *J. Appl. Meteor.,* **35,** 2091–2103.

Gao, W., 1995: Parameterization of subgrid-scale land surface fluxes with emphasis on distributing mean atmospheric forcing and using satellite-derived vegetation index. *J. Geophys. Res.,* **100,** 14 305–14 317.

——, R. L. Coulter, B. M. Lesht, J. Qiu, and M. L. Wesely, 1998: Estimating clear-sky regional surface fluxes in the southern Great Plains Atmospheric Radiation Measurement site with ground measurements and satellite observations. *J. Appl. Meteor.,* **37,** 5–22.

Hirabayashi, Y., S. Seto, T. Oki, S. Kanae, and K. Musiake, 2001: Simulated rainfall in a GCM with retrieved root-zone soil moisture from surface soil moisture estimated with TRMM/PR over the Tropics. *Proc. Fifth Int. Study Conf. on GEWEX in Asia and GAME*, Nagoya, Japan, IAHS, 762–767.

Jackson, R. B., J. Canadell Jr., H. A. Ehleringer, O. E. Mooney, O. E. Sala, and E. D. Schulze, 1996: A global analysis of root distributions for terrestrial biomes. *Oecologia,* **108,** 389–411.

LeMone, M. A., and Coauthors, 2000: Land–atmosphere interaction research, early results, and opportunities in the Walnut River Watershed in southeast Kansas: CASES and ABLE. *Bull. Amer. Meteor. Soc.,* **81,** 757–779.

Mahrt, L., and M. Ek, 1984: The influence of atmospheric stability on potential evaporation. *J. Climate Appl. Meteor.,* **23,** 222–234.

——, and H. L. Pan, 1984: A two-layer model of soil hydrology. *Bound.-Layer Meteor.,* **29,** 1–20.

Mecikalski, J. R., G. R. Diak, M. C. Anderson, and J. M. Norman, 1999: Estimating fluxes on continental scales using remotely sensed data in an atmospheric–land exchange model. *J. Appl. Meteor.,* **38,** 1352–1369.

Miller, M. A., D. T. Troyan, N. L. Miller, J. Jin, S. Kemball-Cook, and K. R. Costigan, 2003: Water cycle variability over a small watershed: A one month comparison of measured and modeled precipitation over the southern Great Plains. *Extended Abstracts, Observing and Understanding the Variability of Water in Weather and Climate*, Long Beach, CA, Amer. Meteor. Soc., CD-ROM, 4.8.

Miller, N. L., and Coauthors, 2005: The DOE Water Cycle Pilot Study. *Bull. Amer. Meteor. Soc.,* **86,** 359–374.

Pan, H. L., and L. Mahrt, 1987: Interaction between soil hydrology and boundary layer development. *Bound.-Layer Meteor.,* **38,** 185–202.

Pitman, A. J., Z. L. Yang, and A. Henderson-Sellers, 1993: Subgrid scale precipitation in AGCMs: Re-assessing the land surface sensitivity using a single column model. *Climate Dyn.,* **9,** 33–41.

Sellers, P. J., F. G. Hall, G. Asrar, D. E. Strebel, and R. E. Murphy, 1988: The First ISLSCP Field Experiment (FIFE). *Bull. Amer. Meteor. Soc.,* **69,** 22–27.

Seth, A., F. Giorgi, and R. E. Dickinson, 1994: Simulating fluxes from heterogeneous land surfaces: Explicit subgrid method employing the biosphere-atmosphere transfer scheme (BATS). *J. Geophys. Res.,* **99,** 18 651–18 667.

Song, J., C. J. Willmott, and B. Hanson, 1997: Influence of heterogeneous land surfaces on surface energy and mass fluxes. *Theor. Appl. Climatol.,* **58,** 175–188.

——, M. L. Wesely, R. L. Coulter, and E. A. Brandes, 2000a: Estimating watershed evapotranspiration with PASS. Part I: Inferring root-zone moisture conditions using satellite data. *J. Hydrometeor.,* **1,** 447–461.

——, ——, M. A. LeMone, and R. L. Grossman, 2000b: Estimating watershed evapotranspiration with PASS. Part II: Moisture budget during drydown periods. *J. Hydrometeor.,* **1,** 462–473.

SSURGO, 1995: Soil Survey Geographic (SSURGO) Database. U.S. Department of Agriculture. [Available online at http://www.ncgc.nrcs.usda.gov/products/datasets/ssurgo and from National Cartography and GIS Center, USDA, National Resource Conservation Service, P.O. Box 6567, Fort Worth, TX 76115.]

Weckwerth, T., and Coauthors, 2004: An overview of the International H2O Project (IHOP_2002) and some preliminary highlights. *Bull. Amer. Meteor. Soc.,* **85,** 253–277.

Yates, D. N., F. Chen, M. LeMone, R. Qualls, S. Oncley, R. Grossman, and E. Brandes, 2001: A Cooperative Atmospheric–Surface Exchange Study (CASES) dataset for analyzing and parameterizing the effects of land surface heterogeneity on area-averaged surface heat fluxes. *J. Appl. Meteor.,* **40,** 921–937.